

Dartmouth College

## Dartmouth Digital Commons

---

Dartmouth Scholarship

Faculty Work

---

7-29-2008

### Chloroplast Fe(III) Chelate Reductase Activity Is Essential for Seedling Viability Under Iron Limiting Conditions

Jeeyon Jeong  
*Dartmouth College*

Christopher Cochu  
*Colorado State University*


Loubna Kerkeb  
*University of South Carolina*

Marinus Pilon  
*Colorado State University*

Erin L. Connolly  
*University of South Carolina*

*See next page for additional authors*

Follow this and additional works at: <https://digitalcommons.dartmouth.edu/facoa>

 Part of the [Biology Commons](#), and the [Plant Sciences Commons](#)

---

#### Dartmouth Digital Commons Citation

Jeong, Jeeyon; Cochu, Christopher; Kerkeb, Loubna; Pilon, Marinus; Connolly, Erin L.; and Guerinot, Mary Lou, "Chloroplast Fe(III) Chelate Reductase Activity Is Essential for Seedling Viability Under Iron Limiting Conditions" (2008). *Dartmouth Scholarship*. 1475.  
<https://digitalcommons.dartmouth.edu/facoa/1475>

This Article is brought to you for free and open access by the Faculty Work at Dartmouth Digital Commons. It has been accepted for inclusion in Dartmouth Scholarship by an authorized administrator of Dartmouth Digital Commons. For more information, please contact [dartmouthdigitalcommons@groups.dartmouth.edu](mailto:dartmouthdigitalcommons@groups.dartmouth.edu).

---

**Authors**

Jeeyon Jeong, Christopher Cohu, Loubna Kerkeb, Marinus Pilon, Erin L. Connolly, and Mary Lou Guerinot

# Chloroplast Fe(III) chelate reductase activity is essential for seedling viability under iron limiting conditions

Jeeyon Jeong\*, Christopher Cohu†, Loubna Kerkeb‡, Marinus Pilon†, Erin L. Connolly‡, and Mary Lou Guerinot\*<sup>§</sup>

\*Department of Biological Sciences, Dartmouth College, Hanover, NH 03755; †Department of Biology, Colorado State University, Fort Collins, CO 80523; and ‡Department of Biological Sciences, University of South Carolina, Columbia, SC 29208

Edited by Maarten J. Chrispeels, University of California at San Diego, La Jolla, CA, and approved May 3, 2008 (received for review September 28, 2007)

**Photosynthesis, heme biosynthesis, and Fe-S cluster assembly all take place in the chloroplast, and all require iron. Reduction of iron via a membrane-bound Fe(III) chelate reductase is required before iron transport across membranes in a variety of systems, but to date there has been no definitive genetic proof that chloroplasts have such a reduction system. Here we report that one of the eight members of the *Arabidopsis* ferric reductase oxidase (FRO) family, FRO7, localizes to the chloroplast. Chloroplasts prepared from *fro7* loss-of-function mutants have 75% less Fe(III) chelate reductase activity and contain 33% less iron per microgram of chlorophyll than wild-type chloroplasts. This decreased iron content is presumably responsible for the observed defects in photosynthetic electron transport. When germinated in alkaline soil, *fro7* seedlings show severe chlorosis and die without setting seed unless watered with high levels of soluble iron. Overall, our results provide molecular evidence that FRO7 plays a role in chloroplast iron acquisition and is required for efficient photosynthesis in young seedlings and for survival under iron-limiting conditions.**

metal homeostasis | FRO | *Arabidopsis* | alkaline soil | photosynthesis

As photosynthetic organisms, plants have an additional need for iron because iron serves as a cofactor in the photosynthetic electron transport chain and is essential for chlorophyll biosynthesis. Indeed, chloroplasts contain up to 90% of the iron found in leaf cells, with about half in the stroma and the rest in the thylakoid membranes (1–4). Despite the quantitative and qualitative significance of iron in chloroplasts, our understanding of iron transport and homeostasis in this organelle is limited.

Plant cells use two distinct mechanisms to acquire iron: one based on chelation and one based on reduction. For initial uptake from the rhizosphere, grasses release phytosiderophores (PSs) that chelate Fe(III); the PS-Fe(III) complexes are then transported into root cells via a plasma membrane transporter in a mechanism known as Strategy II (5). Nongrasses use Strategy I, which utilizes proton release to help solubilize Fe(III), a membrane-bound Fe(III) chelate reductase to convert Fe(III) to the more soluble Fe(II), and a Fe(II)-specific transporter for uptake across the plasma membrane (5). Although grasses can also take up Fe(II) (6), they do not induce proton ATPase activity or Fe(III) chelate reductase activity under iron deficiency as do Strategy I plants.

Once iron has entered the plant, both nicotianamine and citrate have been proposed to serve as iron chelators; mutants that do not either make or transport these chelators properly have iron phenotypes (7). Physiological studies also support the idea of a reduction-based iron acquisition system in leaf cells as well as organelles (8). Fe(III) chelate reductase activities have been detected in leaf disks (9, 10) and leaf protoplasts (11, 12), and inhibition of iron transport into barley chloroplasts by an Fe(II) chelator implicated Fe(III) reduction in plastid transmembrane iron influx (13). Indeed, Fe(II) transport across the chloroplast inner envelope has been detected *in vitro* with inner envelope vesicles (14). Recently, permease in chloroplasts

(PIC1) was proposed to transport iron into chloroplasts (15). Cyanobacterial orthologs of PIC1 belong to clusters of orthologous groups that are generally involved in ion or solute transport in bacteria (15). Although PIC1 was also reported to be part of the chloroplast inner envelope translocon (16), expression of *PIC1* complements the phenotype of a yeast mutant defective in iron uptake, and *pic1* mutants show severe chlorosis, only grow heterotrophically, and accumulate ferritin—all phenotypes consistent with a defect in iron transport. However, it is unknown whether Fe(II) or Fe(III) is transported by PIC1 and whether a Fe(III) chelate reductase is required. There are two possible candidates for a chloroplast-localized reductase in *Arabidopsis*, *FRO6* (At5g49730) and *FRO7* (At5g49740) (17). *FRO6* and *FRO7* are paralogs located in tandem on chromosome 5 that belong to the same eight-member FRO family as the major root Fe(III) chelate reductase, FRO2 (17–20). The conserved functional motifs found in *FRO6* and *FRO7* strongly suggest that *FRO6* and *FRO7* function to reduce Fe(III) chelates [supporting information (SI) Fig. S1]. The proteins show 87% identity and 91% similarity, with the only variable region limited to their N termini (Fig. S1), which leads to a higher score for the predicted chloroplast transit peptide in *FRO7* (21).

In this study, we show that *FRO7* is a chloroplast Fe(III) chelate reductase involved in chloroplast iron homeostasis in young seedlings and is required for survival under iron-limiting conditions. Because *FRO7* localized to the chloroplast whereas *FRO6* was localized on the plasma membrane, we focused on *FRO7* and showed that *FRO7* is highly expressed in photosynthetic tissue, especially younger tissues. Chloroplasts isolated from *fro7* loss-of-function mutant plants have significantly reduced Fe(III) chelate reductase activity, reduced iron content, and altered photosynthetic complexes, providing genetic proof that chloroplasts do rely in part on a reductive strategy for iron acquisition.

## Results

**Localization and Functional Characterization of FRO6 and FRO7 in Yeast.** We constructed C-terminal GFP-fusions of *FRO6* and *FRO7* and examined their subcellular localization in yeast using confocal microscopy. *FRO6*-GFP was detected along the plasma membrane (Fig. 1 *A* and *B*), whereas *FRO7*-GFP appeared as dots, which colocalized with MitoTracker Red CM-H2XRos (Molecular Probes), a mitochondrial marker (Fig. 1 *C–F*). It is

Author contributions: J.J., M.P., E.L.C., and M.L.G. designed research; J.J., C.C., and L.K. performed research; J.J., M.P., E.L.C., and M.L.G. analyzed data; and J.J. and M.L.G. wrote the paper.

The authors declare no conflict of interest.

This article is a PNAS Direct Submission.

<sup>§</sup>To whom correspondence should be addressed. E-mail: guerinot@dartmouth.edu.

This article contains supporting information online at [www.pnas.org/cgi/content/full/0708367105/DCSupplemental](http://www.pnas.org/cgi/content/full/0708367105/DCSupplemental).

© 2008 by The National Academy of Sciences of the USA

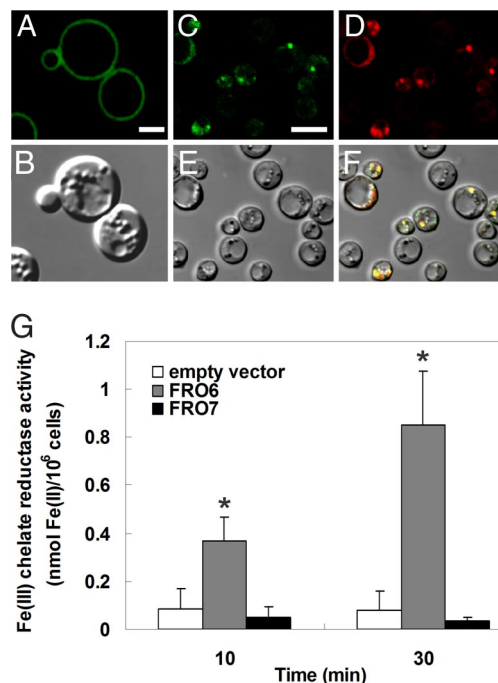


**Fig. 1.** Fe(III) chelate reductase assay and subcellular localization in yeast cells. (A) FRO6-GFP expression. (Scale bar, 2  $\mu$ m.) (B) DIC image of A. (C) FRO7-GFP expression. (Scale bar, 8  $\mu$ m.) (D) FRO7-GFP cells stained with MitoTracker-Red. (E) DIC image of C. (F) Overlay of C–E. (G) Fe(III) chelate reductase activity measured in control cells with an empty vector (white), cells expressing *FRO6* (gray), or *FRO7* (black). Activity of *FRO6*-expressing cells is significantly different from the control cells at both time points. Mean values with SE are shown ( $n = 9$ ). \*,  $P = 0.01$  at 10 min;  $P < 0.01$  at 30 min; Student's  $t$  test.

interesting to note that *FRO7*, which has a predicted chloroplast transit peptide (17), was targeted to mitochondria in yeast cells. Because chloroplast transit peptides are similar to mitochondrial presequences, chloroplast proteins are often targeted to mitochondria when expressed in yeast cells (22). Therefore, the *in silico* predictions and the yeast localization results suggested that *FRO7* would most likely be targeted to chloroplasts in plant cells.

We next performed a Fe(III) chelate reductase assay in yeast. Based on the differential localization of *FRO6* and *FRO7* in yeast, we predicted that Fe(III) chelate reductase activity would be detected for *FRO6* but not for *FRO7* because this assay only measures Fe(III) chelate reductase activity associated with the plasma membrane due to the membrane-impermeant nature of bathophenanthroline disulfonic acid (BPS). The coding regions of *FRO6* and *FRO7* were cloned under the *GAL* promoter and introduced into a wild-type yeast strain. Yeast cells expressing the pea *FRO1* cloned into the same vector were used as a positive control, and cells containing the empty vector were used as a negative control (23). *FRO6*-expressing cells showed up to 5-fold more Fe(III) chelate reductase activity than cells transformed with an empty vector (Fig. 1G). Although the activity of *FRO6*-expressing cells was not as high as that of *PsFRO1*-expressing cells [ $0.9 \pm 0.1$  and  $1.1 \pm 0.2$  nmol Fe(II)/ $10^6$  cells at 10 and 30 min], our result demonstrates that *FRO6* encodes a functional Fe(III) chelate reductase. The Fe(III) chelate reductase activity of *FRO7*-expressing cells did not significantly differ from the basal level observed in the vector-only control cells (Fig. 1G), which is consistent with the internal subcellular localization of *FRO7*. We note that this result contradicts a previous study that reported *FRO7* Fe(III) chelate reductase activity was at least 2.5-fold higher than the negative control, whereas the activity of

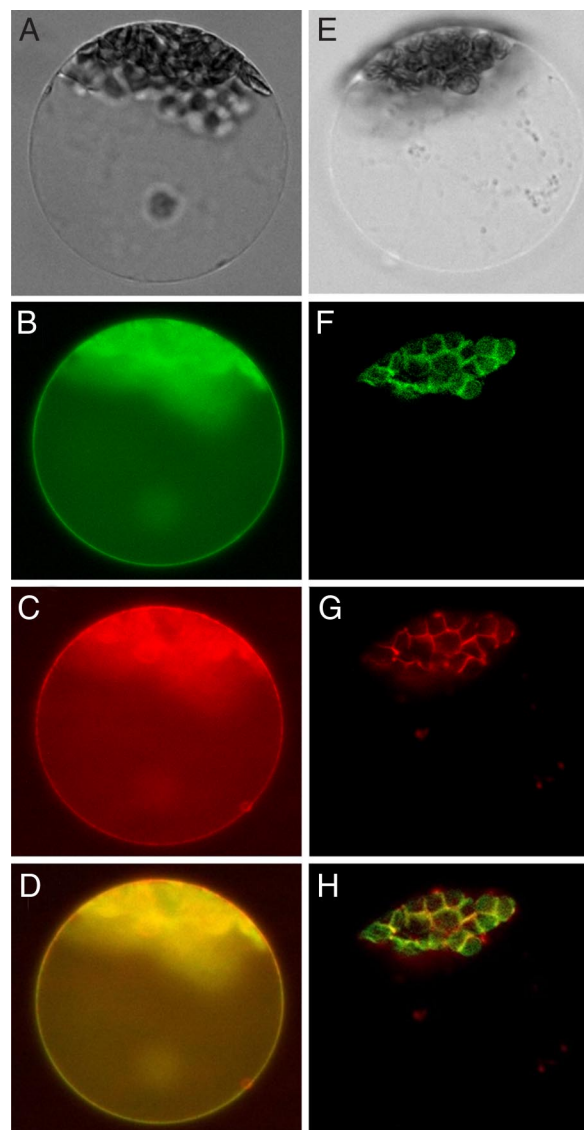


**Fig. 2.** Subcellular localization of *FRO6*-GFP and *FRO7*-GFP in *Arabidopsis* protoplasts. (A) Bright field image of a protoplast cotransformed with *FRO6*-GFP and *AHA2-RFP*. (B) *FRO6*-GFP expression. (C) Expression of the plasma membrane marker, *AHA2-RFP*. (D) Overlay image of B and C. (E) Bright field image of a cell cotransformed with *FRO7*-GFP and *AtOEP7-RFP*. (F) *FRO7*-GFP expression. (G) Expression of the chloroplast membrane marker, *AtOEP7-RFP*. (H) Overlay image of F and G.

*FRO6* was only 20% higher than the negative control (19). However, the activity previously reported for *FRO7* (19) is quite low, i.e., basal level, compared to the levels of Fe(III) chelate reductase activity reported here for *FRO6* and in the *PsFRO1* study (23).

**Localization of *FRO6*-GFP and *FRO7*-GFP in *Arabidopsis* Protoplasts.** To determine the subcellular localization of *FRO6* and *FRO7* in plant cells, we fused GFP to the C terminus of each coding region. The GFP-fusion constructs were cotransformed with a plasma membrane marker, *AHA2-RFP* (24), or a chloroplast marker, *AtOEP7-RFP* (25), into *Arabidopsis* mesophyll protoplasts by PEG transformation (24). Consistent with our yeast localization results, *FRO6*-GFP was detected along the plasma membrane, colocalizing with the plasma membrane marker *AHA2-RFP* (Fig. 2 A–D). Meanwhile, *FRO7*-GFP colocalized

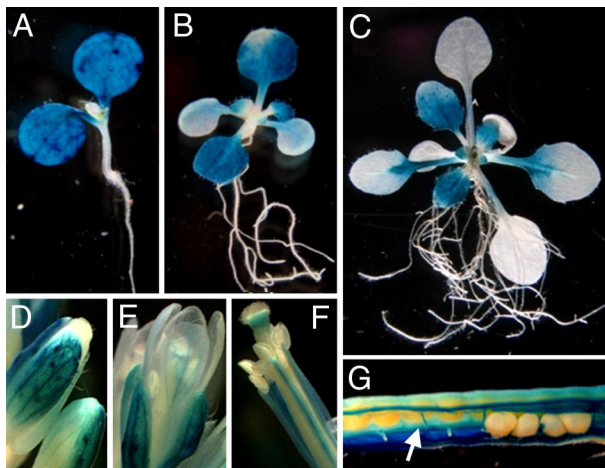


**Fig. 3.** Localization of *FRO7* expression. *FRO7::GUS* expression on day 5 (A), day 10 (B), and day 20 (C). *FRO7::GUS* staining in sepals (D), the veins of petals (E), and the stigma and anther filaments (F). (G) Image of an opened silique showing *FRO7::GUS* expression. A few seeds were removed to capture the staining in funiculi (arrow).

with AtOEP7-RFP (Fig. 2 *E–H*), indicating that the protein was targeted to the chloroplast. Moving forward, we focused on *FRO7* because to our knowledge it is the only *Arabidopsis* FRO family member localized to chloroplasts.

***FRO7::GUS* Is Highly Expressed in the Shoots, Flowers, and Siliques.** To determine where *FRO7* is expressed at the tissue level, we generated transgenic plants expressing the  $\beta$ -glucuronidase (*GUS*) reporter gene fused to the *FRO7* promoter (*FRO7::GUS*). *FRO7::GUS* was expressed in the shoots, but no *GUS* staining was observed in roots (Fig. 3 *A–C*). On day 5 (Fig. 3*A*) and day 10 (Fig. 3*B*), the cotyledons were intensely stained. As the seedlings matured, *FRO7::GUS* expression was restricted to the younger growing leaves, whereas little staining was detected in older mature leaves (Fig. 3*C*). Although shoot-specific expression of *FRO7* was detected by *GUS* staining and quantitative RT-PCR (17, 19), *FRO7::GUS* expression limited to younger growing tissue has not previously been reported. Whereas no staining was observed in the stem or cauline leaves (data not shown), *FRO7::GUS* was expressed in the floral organs, anther filaments, stigma, sepals, and petals (Fig. 3 *D–F*) and in siliques and funiculi (Fig. 3*G*). We note that *FRO6* and *FRO7* are not discriminated on the ATH1 microarray, so that the expression datasets available from Genevestigator (26) and AtGenExpress are composites of *FRO6* and *FRO7* patterns (27).

***fro7* Has Growth Defects When Grown Without Sucrose.** A T-DNA insertion line was obtained from the Salk collection (28) and backcrossed once. We verified the T-DNA insertion 1.3 kb downstream of the ATG within the fifth exon of *FRO7* and confirmed that full-length transcripts of *FRO7* were absent in plants carrying this allele (*fro7*; Fig. S2). Although *fro7* mutants did not show visible growth phenotypes under standard conditions, we observed delayed growth in *fro7* seedlings when germinated with no added sucrose. *fro7* plants germinated without sucrose were smaller, with significantly less shoot-fresh weight than the wild type or the complemented lines (Fig. 4 *A* and *B*). This growth phenotype was partially rescued by supplying sucrose (Fig. 4 *A* and *B*). Because plants grown without sucrose are reliant on photosynthesis, the result suggested that the loss of the chloroplast FRO resulted in reduced photosynthetic efficiency.

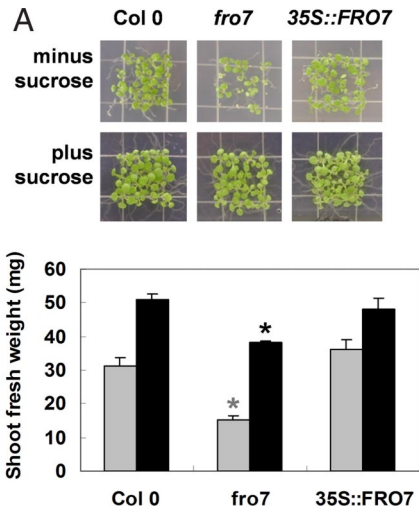


**Fig. 4.** Growth under sucrose deficient conditions. (A) Wild-type (Col 0), *fro7*, and 35S::FRO7 seedlings germinated on sucrose deficient plates on day 14. (B) Shoot fresh weight of each group of seedlings grown on sucrose deficient (gray bars;  $n = 10$ ) or sufficient (black bars;  $n = 9$ ) plates. Mean values with SE are shown. \*,  $P < 0.001$ ; Student's *t* test.

***fro7* Plants Are Defective in Photosynthetic Electron Transport.** To examine photosynthetic electron transport in *fro7* plants, we measured chlorophyll fluorescence of *fro7* seedlings grown on plus- or minus-sucrose plates using a kinetic fluorescence camera (FluorCam). Based on the growth phenotype on minus-sucrose plates, we expected a high chlorophyll fluorescence phenotype in *fro7* seedlings. The flux of electrons through photosystem (PS) II ( $\Phi_{PSII}$ ) and the photochemical quenching coefficient ( $qP$ ), which indicates the proportion of PSII reaction centers that are open, were significantly reduced in *fro7* compared to the wild type under both plus- and minus-sucrose conditions, whereas  $\Phi_{PSII}$  and  $qP$  values of the complemented lines were not significantly different from wild-type plants (Fig. 5*A* and Table S1). The reduction of  $\Phi_{PSII}$  and  $qP$  in *fro7* is statistically significant but not as drastic compared to other photosynthesis mutants such as *paa2* (29).

***fro7* Chloroplasts Have Significantly Reduced Fe(III) Chelate Reductase Activity and Iron Content.** To detect Fe(III) chelate reductase activity on the chloroplast, we isolated chloroplasts from 2-week-old seedlings of wild-type *fro7* and *fro7*-complemented with 35S::FRO7 (referred to as 35S::FRO7) plants and measured Fe(III) chelate reductase activity. Time-course measurements showed that Fe(III) chelate reductase activity of wild-type chloroplasts was saturated within 30 min (data not shown). Chloroplasts isolated from *fro7* plants had 75% less Fe(III) chelate reductase activity compared to wild-type chloroplasts, and the activity of chloroplasts isolated from 35S::FRO7 plants was restored to the wild-type level (Fig. 5*C*). This result provides evidence that Fe(III) chelate reductase activity is present on the chloroplast and that FRO7 is responsible for such activity.

We then carried out elemental analysis of the isolated chloroplasts using inductively coupled plasma-mass spectrometry (ICP-MS). We postulated that the mutant chloroplasts might contain less iron compared to wild-type chloroplasts because the presence of a FRO family member on the chloroplast and Fe(III) chelate reductase activity associated with intact chloroplasts suggested that a reduction strategy is involved in iron uptake into chloroplasts. Although no significant difference was observed in the iron content of *fro7* and wild-type protoplasts, shoots or seeds (Table S2), *fro7* chloroplasts contained 33% less iron than wild-type chloroplasts, whereas the iron content of 35S::FRO7

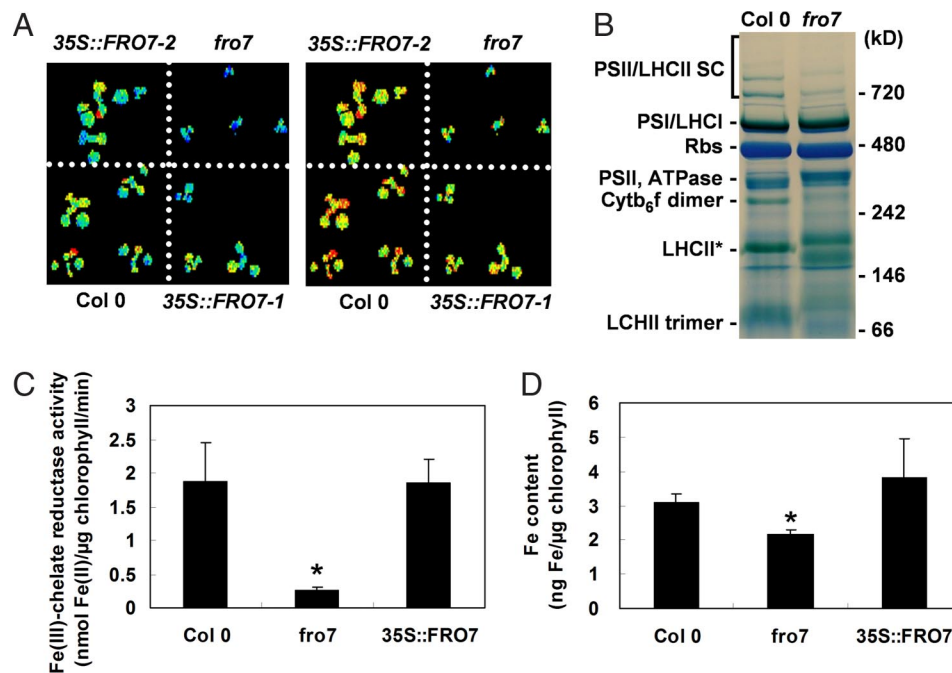


**Fig. 5.** Analyses of *fro7* chloroplasts. (A) Chlorophyll fluorescence measurements. False color images of  $\Phi_{PSII}$  (Left) and  $qP$  (Right) in wild-type (Col 0), *fro7*, and two complemented lines grown on sucrose minus plates. (B) Blue native gel electrophoresis. Protein bands of wild-type photosynthetic complexes are labeled. PSII/LHCII SC, PSII/LHCII supercomplex; Rbs, ribulose-1,5-bisphosphate carboxylase/oxygenase. (C) Fe(III) chelate reductase activity of chloroplasts isolated from Col 0, *fro7*, and 35S::FRO7 lines. Mean values with SE at 30 min are shown ( $n = 6$ ). (D) Iron content of chloroplasts harvested from Col 0, *fro7*, and 35S::FRO7 lines. Mean values with SE are shown ( $n = 7$ ). \*,  $P < 0.05$ ; Student's  $t$  test.

chloroplasts was not significantly different from wild-type chloroplasts (Fig. 5D). The content of other metals, such as copper, manganese, or zinc, was not significantly different in *fro7* and wild-type plants (data not shown).

**Photosynthetic Complexes Are Altered in *fro7* Chloroplasts.** Based on the defects in photosynthetic electron transport and reduced chloroplast iron content in the mutant line, we hypothesized that the assembly of photosynthetic complexes might be affected in *fro7*. Thus, we carried out blue native gel electrophoresis with wild-type or *fro7* chloroplast proteins solubilized with 1% *n*-dodecyl- $\beta$ -D-maltoside. *fro7* chloroplasts had reduced levels of cytochrome  $b_6f$  (cyt $b_6f$ ) dimers compared to wild-type chloroplasts (Fig. 5B). Cyt $b_6f$  is the second-largest sink for iron in the photosynthetic apparatus with four hemes and one Fe $_2$ -S $_2$  cluster (30). Although the largest sink for iron in the photosynthetic apparatus is photosystem I (PSI) with three Fe $_4$ -S $_4$  clusters (31), PSI levels were similar in *fro7* compared to wild type. Meanwhile, the supercomplexes made of the light harvesting complex II (LHCII) and PSII (PSII/LHCII) were down-regulated, and LHCII itself was also affected in *fro7*, showing two distinct bands instead of the single band observed in wild type (Fig. 5B). PSII contains two cytochromes and one nonheme iron (32); LHCII is the most abundant chlorophyll-protein complex in thylakoids of higher plants, and most of the chlorophyll *b* is associated with this complex (33). Despite the changes in photosynthetic complexes, chlorophyll *a* and *b*, and carotenoid content of *fro7* were not significantly different from that of wild-type plants (data not shown).

***fro7* Has Growth Defects in Alkaline Soil.** If FRO7 is involved in iron transport into chloroplasts, we postulated that *fro7* mutants would be more susceptible to iron deficiency than wild-type plants. To test the hypothesis, we germinated wild-type, *fro7*, and 35S::FRO7 lines in alkaline soil (pH 8) where the availability of iron is limited (34). By day 14, *fro7* seedlings showed severe

chlorosis and growth defects, whereas the wild-type and complemented lines were only slightly chlorotic (Fig. 6). The phenotype was rescued by watering with excess soluble iron (Fig. 6). This result suggested that chloroplast Fe(III) chelate reductase activity is essential for survival of young seedlings under iron-limiting conditions.

## Discussion

The family of metalloreductases to which the *Arabidopsis* FRO proteins belong is found in a wide range of organisms, including fungi, plants, and mammals. Although the majority of the family members characterized to date have been localized to the plasma membrane, there are now several recent studies showing localization of metalloreductases to internal membranes. In yeast, the FRE6 metalloreductase localizes to the vacuolar membrane and functions in Ctr2-mediated vacuolar copper transport (35) as

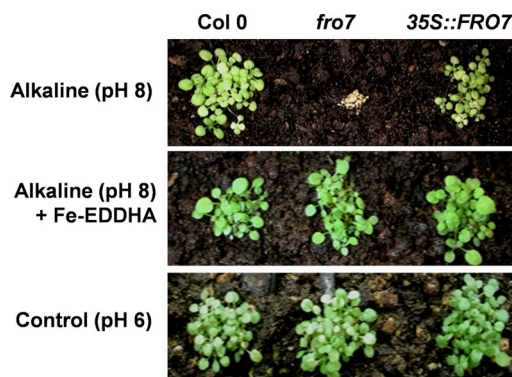


**Fig. 6.** Germination in alkaline soil. Col 0, *fro7*, and 35S::FRO7 plants germinated in alkaline soil (pH 8.0) with or without Fe-EDDHA watering and control soil (pH 6) on day 14.

well as in Fe(II) transport by Smf3 and the Fet5/Fth1 complex (36), similar to the way that the FRE1 metalloredoxase functions with iron and copper transporters at the plasma membrane. The four putative metalloredoxases in mammals, STEAP1–4, all at least partially colocalize with transferrin and transferrin receptor to endosomes, where Fe(III) must be reduced before it is transported out of the endosomes by divalent metal transporter 1 (37, 38). Our localization of FRO7 to the chloroplast expands the list of internally localized metalloredoxases and suggests that iron movement across the chloroplast membrane is mechanistically similar to that of other membranes.

As FRO7 is not iron-regulated (17), it is unlikely that its main role is to supply iron to chloroplasts under conditions that induce the Strategy I response. Rather, based on the expression pattern of FRO7, we propose that FRO7 is more likely involved in supplying iron to chloroplasts of young growing tissues in response to developmental cues. This pattern of expression differs from that of the presumptive iron transporter, PIC1, which is constitutively and ubiquitously expressed throughout the plant's life cycle (15). Such contrasting expression patterns may explain why *fro7* plants are not as severely affected as *pic1* mutants when iron is not limiting. When iron is limiting, *fro7* mutants die as seedlings, just like *pic1* mutants. However, unlike *pic1* mutants, *fro7* mutants can be rescued by supplying high levels of soluble iron. This suggests that there are partially redundant systems for iron uptake into the chloroplast that can bypass FRO7 but not PIC1. No other FRO family members localize to the chloroplast, so the other uptake system may not require a reduction step. Because a severe phenotype is seen only when iron is limiting, it suggests the alternative uptake system has a lower affinity for iron than the FRO7-associated system.

Although it is not yet known whether PIC1 transports Fe(II) or Fe(III), we speculate that chloroplasts might take up both Fe(II) and Fe(III) via multiple pathways as observed in modern day cyanobacteria. In the cyanobacteria *Synechocystis* sp. PCC 6803, Fe(III) is mainly transported by an ATP-binding cassette transporter, FutABC (39). It was also reported that at least two Fe(II) uptake systems were responsible for Fe(II) uptake in the *fut* mutants or when the cells were under iron deficiency (39). To our knowledge, no membrane-bound ferric chelate reductase has been characterized in cyanobacteria. However, a BLAST search against CyanoBase (40) revealed that orthologs of FRO7 are present in cyanobacteria, including a predicted Fe(III) reductase from *Anabaena variabilis* ATCC 29413 with  $\approx 20\%$  identity and 40% similarity to FRO7.

There have been a number of detailed studies on the changes seen in the photosynthetic apparatus in response to iron deficiency. In *Chlamydomonas*, studies have shown that there is proteolytic loss of both photosystems as well as of the Cyt<sub>b</sub><sub>6</sub>f complex (41, 42). The thylakoid proteome of sugar beet showed significant changes in response to iron deficiency, with the relative amount of electron transfer complexes reduced (43). Because *fro7* plants were less efficient in photosynthetic electron transport (Fig. 5A and Table S1) and their chloroplasts contained significantly less iron (Fig. 5D), a major cofactor of photosynthetic complexes, we postulated that the assembly of photosynthetic apparatus might be altered in *fro7*. Consistent with our hypothesis, we found striking differences between *fro7* and wild-type photosynthetic complexes (Fig. 5B). In particular, the dramatic reduction of Cyt<sub>b</sub><sub>6</sub>f complex levels (Fig. 5B) agrees with the kinetic profile of *fro7* chlorophyll fluorescence, which suggested that PSII was functional and that the defect was more likely a downstream effect (data not shown). We note that the photosynthetic complexes affected in *fro7* contain heme, whereas the hemeless PSI was not greatly affected by loss of FRO7. This may reflect the fact that plastids are thought to be the major site of heme biosynthesis

(44), whereas Fe-S clusters are assembled in both plastids and mitochondria (45).

In summary, our study shows that FRO7 is a chloroplast Fe(III) chelate reductase required for survival under iron-limiting conditions, for efficient photosynthesis, and for proper chloroplast iron acquisition in young seedlings.

## Materials and Methods

**Localization in Yeast.** FRO6-GFP or FRO7-GFP transformants were grown with 2% galactose, harvested at mid-log phase, and examined under a confocal microscope, Leica TSC-SP UV. For colocalization with mitochondria, cells were stained with MitoTracker Red CM-H2XRos (Molecular Probes) as described (46).

**Yeast Fe(III) Chelate Reductase Assay.** Yeast transformants were grown on 2% galactose to induce expression of FRO6 or FRO7 and 10  $\mu$ M FeCl<sub>3</sub> to repress endogenous Fe(III)-chelate reductase activities and harvested at mid-log phase (23). The cells were incubated at 30°C in low-iron medium without EDTA containing 100  $\mu$ M FeCl<sub>3</sub> and 1 mM BPS. Fe(III) chelate reductase activity was quantified based on the absorbance measured at 520 nm (23, 47).

**Transient Expression in Arabidopsis Protoplasts.** Protoplasts were isolated and cotransformed with FRO6-GFP or FRO7-GFP with RFP markers by the PEG method (24) and examined after 16–32 h. Fluorescence images were captured with an epifluorescence microscope, Nikon Eclipse 80i, using filter sets 31001 (exciter: D480/20x, dichroic: 505DCLP, emitter: D535/40m) for GFP and 31003 (exciter: D546/10x, dichroic: 560DCLP, emitter: D590/30m) for RFP from Chroma Technology Corporation.

**Fluorescence Measurements.** Chlorophyll fluorescence was imaged by using a FluorCam 700MF controlled by version 5.0 PSI Fluorcam software Quenching Analysis (Photon Systems Instruments) with actinic light at 150  $\mu$ mol of photons $\cdot$ m<sup>-2</sup> $\cdot$ s<sup>-1</sup> and saturating pulse intensity at 100% on overnight dark-adapted plants. All parameters have been normalized for the plant size within the software. Plants were grown in 1/2MS (48) and 0.7% agarose for 14 days in 12 h of light at 120  $\mu$ mol of photons $\cdot$ m<sup>-2</sup> $\cdot$ s<sup>-1</sup> and 23°C.

**Chloroplast Fe(III) Chelate Reductase Assay.** Two-week-old seedlings grown on B5 plates with 12 h of light at 22°C were used for protoplast isolation, and biochemically active chloroplasts were isolated by rupturing the protoplasts and centrifuging on a 40%/85% percoll step gradient as described (49). Purity of chloroplast fractions was checked by Western blots with antibodies against  $\alpha$ -tubulin and IscA (Fig. 53), and the intactness of isolated chloroplasts were assessed based on the ratio of Rubisco large subunit, Rubisco small subunit, and light-harvesting chlorophyll-binding protein in total homogenate versus isolated chloroplasts ( $\approx 90\%$ ) (data not shown). Fe(III) chelate reductase assays were carried out with light at 60  $\mu$ E $\cdot$ m<sup>-2</sup> $\cdot$ sec<sup>-1</sup> using chloroplasts equivalent to 0.1–0.15 mg of chlorophyll per reaction, with 300  $\mu$ M ferrozine and 100  $\mu$ M Fe-EDTA in Hepes-sorbitol buffer (pH 7.3).

**Elemental Analysis.** Chloroplasts were isolated as described above and vacuum-dried in a speed vac. Elemental analysis was done by ICP-MS at Purdue University as described (50). Chloroplasts equivalent to 30  $\mu$ g of chlorophyll were used.

**Blue Native Gel Electrophoresis.** Blue native gel electrophoresis with chloroplast protein samples was carried out as described (51, 52). Chloroplasts were solubilized in 50 mM Bis-Tris-HCl (pH 7.0), 0.5 M *n*-aminocaproic acid, and 10% (wt/vol) glycerol containing 1% *n*-dodecyl- $\beta$ -D-maltoside. The samples were incubated on ice for 10 min and centrifuged at 100,000  $\times$  g for 10 min at 4°C. Samples corresponding to 50  $\mu$ g of protein were separated on NativePAGE Novex 4–16% Bis-Tris gels (Invitrogen). Protein bands corresponding to different photosynthetic complexes were determined based on their molecular masses (51, 53). NativeMark Unstained Protein Standard (Invitrogen) was used for molecular weight estimation.

Further details are available in *SI Materials and Methods*.

**ACKNOWLEDGMENTS.** We thank Rob McClung and Joohyun Lee for critically reading the manuscript; David Salt, Ivan Baxter, and Brett Lahner for ICP-MS; Danny Schnell and Fei Wang for technical help with chloroplast isolation; and Inhwan Hwang (POSTECH, Korea) for providing the vector and RFP markers for transient expression. This work was supported by National Science Foundation Grants IBN-0344305 (to M.L.G. and E.L.C.) and IBN-0418993 (to M.P.).

1. Terry N, Abadia J (1986) Function of iron in chloroplasts. *J Plant Nutr* 9:609–646.
2. Landsberg E (1984) Regulation of iron-stress-response by whole-plant activity. *J Plant Nutr* 7:609–621.
3. Bughio N, Takahashi M, Yoshimura E, Nishizawa NK, Mori S (1997) Light-dependent iron transport into isolated barley chloroplasts. *Plant Cell Physiol* 116:1063–1072.
4. Shikanai T, Müller-Moulé P, Munekega Y, Niyogi KK, Pilon M (2003) PAA1, a P-type ATPase of Arabidopsis, functions in copper transport in chloroplasts. *Plant Cell* 15:1333–1346.
5. Grotz N, Guerinot ML (2006) Molecular aspects of Cu, Fe and Zn homeostasis in plants. *Biochim Biophys Acta* 1763:595–608.
6. Ishimaru Y, et al. (2006) Rice plants take up iron as an Fe<sup>3+</sup>-phytosiderophore and as Fe<sup>2+</sup>. *Plant J* 45:335–346.
7. Briat JF, Curie C, Gaymard F (2007) Iron utilization and metabolism in plants. *Curr Opin Plant Biol* 10:276–282.
8. Moog PR, Brüggemann W (1994) Iron reductase systems on the plant plasma membrane—A review. *Plant Soil* 165:241–260.
9. Larbi A, et al. (2001) Technical advance: Reduction of Fe(III)-chelates by mesophyll leaf disks of sugar beet. Multi-component origin and effects of Fe deficiency. *Plant Cell Physiol* 42:94–105.
10. de la Guardia MD, Alcázar E (1996) Ferric chelate reduction by sunflower (*Helianthus annuus* L.) leaves: Influence of light, oxygen, iron-deficiency and leaf age. *J Exp Bot* 47:669–675.
11. Gonzalez-Vallejo EB, Morales F, Cistue L, Abadia A, Abadia J (2000) Iron deficiency decreases the Fe(III)-chelate reducing activity of leaf protoplasts. *Plant Physiol* 122:337–344.
12. Brüggemann W, Maas-Kantel K, Moog PR (1993) Iron uptake by leaf mesophyll cells: The role of the plasma membrane-bound ferric-chelate reductase. *Planta* 190:151–155.
13. Bughio N, Takahashi M, Yoshimura E, Nishizawa NK, Mori S (1997) Characteristics of light-regulated iron transport system in barley chloroplasts. *Soil Sci Plant Nutr* 43:959–963.
14. Shingles R, North M, McCarty RE (2002) Ferrous ion transport across chloroplast inner envelope membranes. *Plant Physiol* 128:1022–1030.
15. Duy D, et al. (2007) PIC1, an ancient permease in Arabidopsis chloroplasts, mediates iron transport. *Plant Cell* 19:986–1006.
16. Teng YS, et al. (2006) Tic21 is an essential translocon component for protein translocation across the chloroplast inner envelope membrane. *Plant Cell* 18:2247–2257.
17. Mukherjee I, Campbell NH, Ash JS, Connolly EL (2006) Expression profiling of the Arabidopsis ferric chelate reductase (*FRO*) gene family reveals differential regulation by iron and copper. *Planta* 223:1178–1190.
18. Robinson NJ, Procter CM, Connolly EL, Guerinot ML (1999) A ferric-chelate reductase for iron uptake from soils. *Nature* 397:694–697.
19. Wu H, et al. (2005) Molecular and biochemical characterization of the Fe(III) chelate reductase gene family in Arabidopsis thaliana. *Plant Cell Physiol* 46:1505–1514.
20. Feng H, et al. (2006) Light-regulated, tissue-specific, and cell differentiation-specific expression of the Arabidopsis Fe(III)-chelate reductase gene AtFRO6. *Plant Physiol* 140:1345–1354.
21. Schwacke R, et al. (2003) ARAMEMNON, a novel database for Arabidopsis integral membrane proteins. *Plant Physiol* 131:16–26.
22. Versaw WK, Harrison MJ (2002) A chloroplast phosphate transporter, PHT2;1, influences allocation of phosphate within the plant and phosphate-starvation responses. *Plant Cell* 14:1751–1766.
23. Waters BM, Blevins DG, Eide DJ (2002) Characterization of FRO1, a pea ferric-chelate reductase involved in root iron acquisition. *Plant Physiol* 129:85–94.
24. Kim DH, et al. (2001) Trafficking of phosphatidylinositol 3-phosphate from the trans-Golgi network to the lumen of the central vacuole in plant cells. *Plant Cell* 13:287–301.
25. Lee KH, Kim SJ, Lee YJ, Jin JB, Hwang I (2003) The M domain of atToc159 plays an essential role in the import of proteins into chloroplasts and chloroplast biogenesis. *J Biol Chem* 278:36794–36805.
26. Zimmermann P, Hirsch-Hoffmann M, Hennig L, Gruissem W (2004) GENEVESTIGATOR. Arabidopsis microarray database and analysis toolbox. *Plant Physiol* 136:2621–2632.
27. Schmid M, et al. (2005) A gene expression map of Arabidopsis thaliana development. *Nat Genet* 37:501–506.
28. Alonso JM, et al. (2003) Genome-wide insertional mutagenesis of Arabidopsis thaliana. *Science* 301:653–657.
29. Abdel-Ghany SE, Muller-Moule P, Niyogi KK, Pilon M, Shikanai T (2005) Two P-type ATPases are required for copper delivery in Arabidopsis thaliana chloroplasts. *Plant Cell* 17:1233–1251.
30. Kurisu G, Zhang H, Smith JL, Cramer WA (2003) Structure of the cytochrome b6f complex of oxygenic photosynthesis: Tuning the cavity. *Science* 302:1009–1014.
31. Jordan P, et al. (2001) Three-dimensional structure of cyanobacterial Photosystem I at 2.5 Å resolution. *Nature* 411:909–917.
32. Zouni A, et al. (2001) Crystal structure of Photosystem II from *Synechococcus elongatus* at 3.8 Å resolution. *Nature* 409:739–743.
33. Bassi R, Hoyer-Hansen G, Barbato R, Giacometti GM, Simpson DJ (1987) Chlorophyll-proteins of the photosystem II antenna system. *J Biol Chem* 262:13333–13341.
34. Kim SA, et al. (2006) Localization of iron in Arabidopsis seed requires the vacuolar membrane transporter VIT1. *Science* 314:1295–1298.
35. Rees EM, Thiele DJ (2007) Identification of a vacuole-associated metallo-reductase and its role in Ctr2-mediated intracellular copper mobilization. *J Biol Chem* 282:21629–21638.
36. Singh A, Kaur N, Kosman DJ (2007) The metallo-reductase Fre6p in Fe-efflux from the yeast vacuole. *J Biol Chem* 282:28619–28626.
37. Ohgami RS, et al. (2005) Identification of a ferrireductase required for efficient transferrin-dependent iron uptake in erythroid cells. *Nat Genet* 37:1264–1269.
38. Ohgami RS, Campagna DR, McDonald A, Fleming MD (2006) The Steap proteins are metallo-reductases. *Blood* 108:1388–1394.
39. Katoh H, Hagino N, Grossman AR, Ogawa T (2001) Genes essential to iron transport in the cyanobacterium *Synechocystis* sp. strain PCC 6803. *J Bacteriol* 183:2779–2784.
40. Nakamura Y, Kaneko T, Hirose M, Miyajima N, Tabata S (1998) CyanoBase, a www database containing the complete nucleotide sequence of the genome of *Synechocystis* sp. strain PCC6803. *Nucleic Acids Res* 26:63–67.
41. Moseley JL, Allinger et al. (2002) Adaptation to Fe-deficiency requires remodeling of the photosynthetic apparatus. *EMBO J* 21:6709–6720.
42. Naumann B, Stauber EJ, Busch A, Sommer F, Hippler M (2005) N-terminal processing of Lhc3 is a key step in remodeling of the photosystem I-light-harvesting complex under iron deficiency in *Chlamydomonas reinhardtii*. *J Biol Chem* 280:20431–20441.
43. Andaluz S, et al. (2006) Proteomic profiles of thylakoid membranes and changes in response to iron deficiency. *Photosynth Res* 89:141–155.
44. Tanaka R, Tanaka A (2007) Tetrapyrrole biosynthesis in higher plants. *Annu Rev Plant Biol* 58:321–346.
45. Balk J, Lobreaux S (2005) Biogenesis of iron-sulfur proteins in plants. *Trends Plants Sci* 10:324–331.
46. Burgess SM, Delannoy M, Jensen RE (1994) MMM1 encodes a mitochondrial outer membrane protein essential for establishing and maintaining the structure of yeast mitochondria. *J Cell Biol* 126:1375–1391.
47. Eide D, Davis-Kaplan S, Jordan I, Sipe D, Kaplan J (1992) Regulation of iron uptake in *Saccharomyces cerevisiae*. The ferrireductase and Fe(II) transporter are regulated independently. *J Biol Chem* 267:20774–20812.
48. Murashige T, Skoog F (1962) A revised medium for rapid growth and bio assays with tobacco tissue cultures. *Physiol Plant* 15:473–497.
49. Smith MD, Fitzpatrick L, Keegstra K, Schnell DJ (2002) In vitro analysis of chloroplast protein import. *Current Protocols in Cell Biology*, eds Bonifacino JS, Dasso M, Harford JB, Lippincott-Schwartz J, Yamada KM (Wiley, New York), pp 11.16.1–11.16.21.
50. Lahner B, et al. (2003) Genomic scale profiling of nutrient and trace elements in Arabidopsis thaliana. *Nat Biotechnol* 21:1215–1221.
51. Asakura Y, et al. (2004) Maize mutants lacking chloroplast FtsY exhibit pleiotropic defects in the biogenesis of thylakoid membranes. *Plant Cell* 16:201–214.
52. Schagger H, Cramer WA, Vonjagow G (1994) Analysis of molecular masses and oligomeric states of protein complexes by blue native electrophoresis and dimensional native electrophoresis. *Anal Biochem* 217:220–230.
53. Yabe T, et al. (2004) The Arabidopsis chloroplastic NifU-like protein CnfU, which can act as an iron-sulfur cluster scaffold protein, is required for biogenesis of ferredoxin and photosystem I. *Plant Cell* 16:993–1007.